Damping of Compressible MHD Modes in Magnetically Twisted Flux Tubes

Ioannis Giagkiozis[1], Gary Verth[1], Viktor Fedun[1], Tom Van Doorsselaere[2], Marcel Goossens[2]

[1] University of Sheffield, United Kingdom
[2] University of Leuven – KU Leuven, Belgium

ABSTRACT

Damping due to resonant absorption is absent from sausage modes in magnetic flux tubes with straight magnetic field. However, in presence of internal and external magnetic twist, the Alfven coupling coefficient is no longer zero and as a consequence resonant absorption appears. In this work we study the expected damping times for waves in the Alfven continuum for various solar atmospheric conditions. We obtain a complex dispersion relation and the associated damping times are identified by numerically solving this equation. Based on this model we can explain recent observations of sausage wave damping in the chromosphere.

RESULTS

Model illustration.

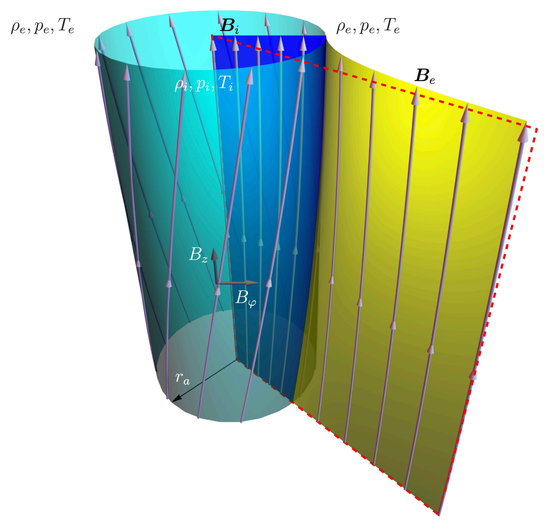

Straight magnetic cylinder with variable twist inside ($r<r_a$) and outside ($r > r_a$), where r_a is the tube radius, ρ_i, p_i and T_i are the density, pressure and temperature at equilibrium inside the tube. The corresponding quantities outside the tube are denoted with a subscript *e*. B_φ is continuous across the tube boundary. The dark blue surface inside the magnetic cylinder represents the influence of $B_\varphi \propto r$. The yellow surface outside the cylinder illustrates the $B_\varphi \propto 1/r$ dependence. The dashed red rectangle represents a magnetic surface with only a longitudinal *(z)* magnetic field component.

Simulations

To excite MHD wave modes in axisymmetric open magnetic flux tube embedded in the realistic solar atmosphere we perturbed the the foot point by various drivers e.g. vertical, horisontal and swirly motion (see e.g. *Fedun, Erdelyi & Shelyag, 2009, SolPhys, Mumford, Fedun & Erdelyi, 2014, ApJ, Shelyag, Fedun, Erdelyi, 2008, A&A and Vigeesh et. al, 2012, ApJ*. Observed vortex drivers naturally lead to twist. 3D these models are confined to the chromosphere. Physically consistent equilibria for both the chromosphere and corona is very challenging.

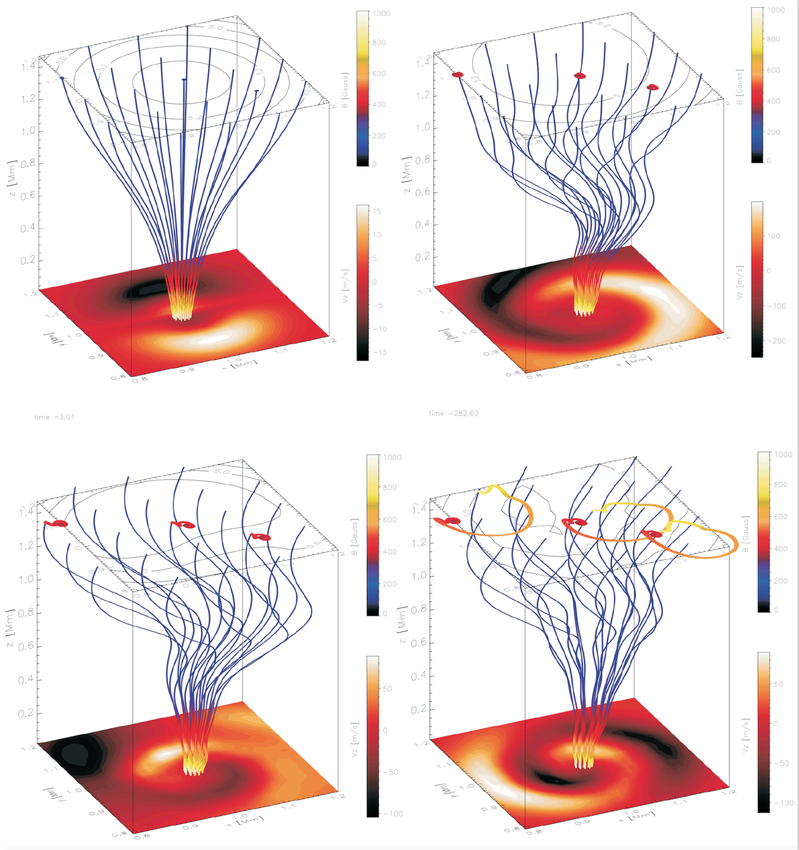

Three-dimensional snapshots of the MHD wave propagation in an open magnetic flux tube are shown. The thin multicolor curves represent the magnetic field lines. The lower and upper color bars correspond to the vertical velocity Vz at the level of the driver location and to the strength value of the magnetic field along the magnetic field lines, respectively. The black iso-contours of the magnetic field labeled by appropriate value of the strength of the magnetic field are shown in the top horizontal slice taken at height h = 1.4 Mm. At the bottom of each snapshot the horizontal cross-cut at the location of the swirl driver is shown. The 3D trajectory of the top ends of the three representative magnetic field lines are shown as colored thick curves.

Magnetic twist

The presence of weak twist changes the character of axisymmetric modes in a significant way as seen in the figure below. Namely, while in the case with no magnetic twist the azimuthal component of the velocity perturbation is zero, in the case with twist this component is almost never zero. This effect is clearly seen, where the relative magnitude of the radial and azimuthal components of the velocity perturbation alternate periodically. Also, given that observations of Alfvén waves rely on the apparent absence of intensity (i.e. density) perturbations in conjunction with torsional motion, we suggest an alternative interpretation. Namely, observed waves that appear to be Alfénic in nature could actually be surface sausage waves (see right panel of the below figure), since due to the localised character of the density perturbation, this perturbation could be below the instrument resolution.

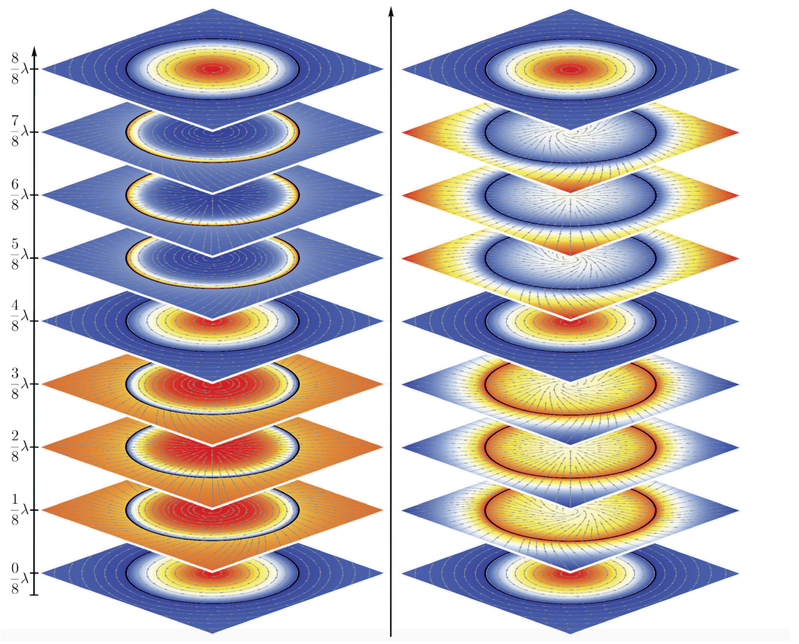

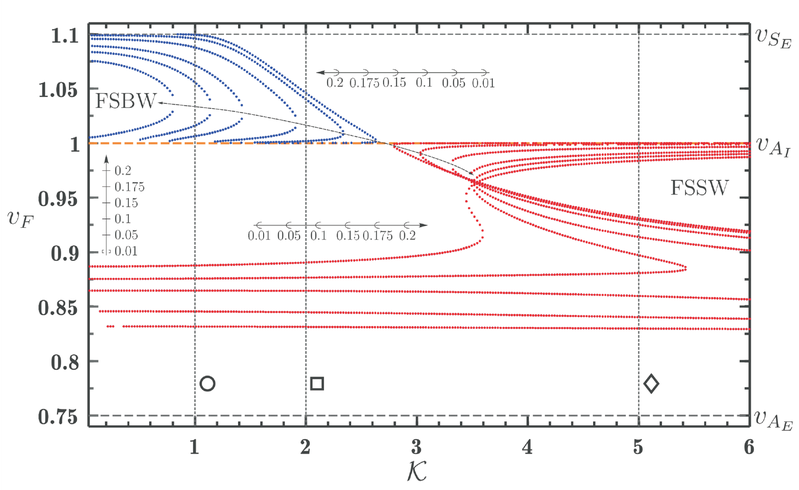

Solutions of the dispersion equation in presence of internal and external twist for a cool evacuated magnetic flux tube embedded in a dense environment ($\beta_i<<1$, $\beta_e>>1$) with speed ordering $V_{Se} > V_{Ai} > V_{Ae} > V_{Si}$.

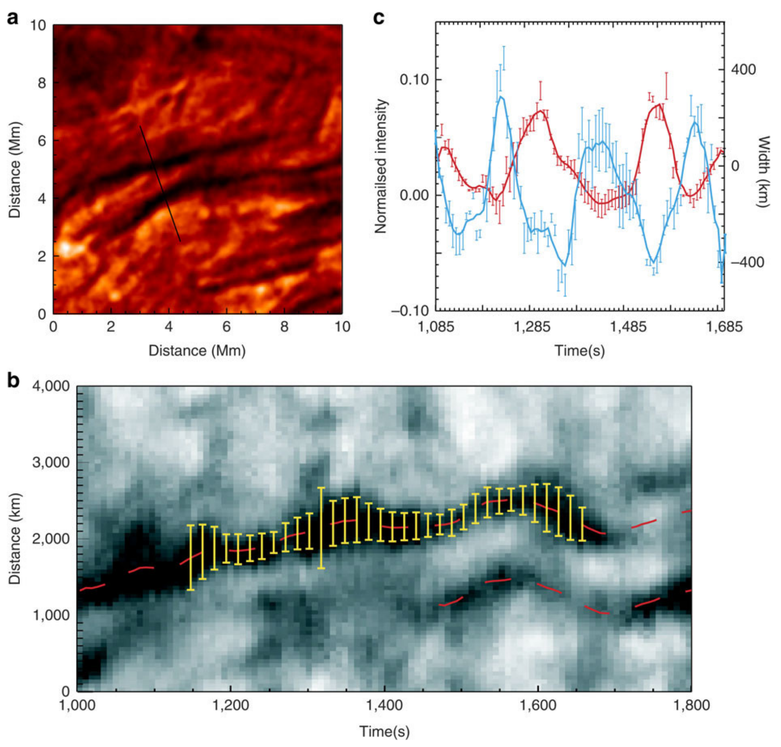

Morton et al. (2012) directly observed ubiquitous sausage waves in chromsopheric fibrils, concurrent with kink waves. Panel (a) depicts a cropped ROSA *Hα* snapshot containing a pair of dark, and hence dense, chromospheric flux tubes. Using the cross-cut (black line) to extract intensity information, panel (b) displays the resulting time--distance diagram revealing the dynamic motion of the waveguides. Times are given in seconds from the start of the data set, while the overplots are the results from a Gaussian fitting routine to show concurrent kink (red line shows the central axis of the structure) and sausage waves (yellow bars show the measured width of structure). Here there are counter-propagating kink waves with periods of
232 ±8 s and phase speeds of 71±22 km/s upwards and 87±26 km/s downwards. The maximum transverse velocity amplitudes in both cases is about 5 km/s. The sausage wave shown here has a period of 197±8 s, a phase speed of 67± 15 km/s and maximum transverse velocity amplitude of 1-2 km/s. Panel (c) displays a comparison between the detected intensity (blue) and width (red) perturbations resulting from the Gaussian fitting. Sausage waves can naturally cause such anti-phase behaviour. Damping of kink waves due to resonant absorption has been well studied in the coronal waveguides, e.g. in post-flare/CME loops (see e.g., *Verwichte et al. 2013*). Now a new era is beginning where we can also start to investigate the damping behaviour of sausage waves in chrosmopheric waveguides.

Dispersion relation for the Alfven continuum

$$\mathcal{D}_1 + i\mathcal{D}_2 = 0$$

$$\mathcal{D}_1 = 2\frac{D_i}{k_{ri}^2}\frac{M(a,b-1;s_i)}{M(a,b;s_i)} - 2\rho_i n_i(n_i+k_z)\frac{v_{A\varphi i}^2}{k_{ri}^2} - \frac{r_i}{r_e k_{re}^2}\left\{(1-\nu)D_e - 2\rho_e n_e^2 v_{A\varphi e}^2\right\}$$

$$\mathcal{D}_2 = \frac{i2\delta_A\pi}{|\rho_e-\rho_i|}\frac{v_{A\varphi B}^2}{v_{AB}^4}\left[\frac{2}{k_{ri}^2}\left(D_i\frac{M(a,b-1;s_i)}{M(a,b;s_i)} - n_i(n_i+k_z)\rho_i v_{A\varphi i}^2\right) + 2\rho_i v_{Ai}^2\right]$$
$$\left[2\frac{B_z^2}{\mu_0 r_A} + \frac{1}{r_e k_{re}^2}\left\{(1-\nu)D_e - 2\rho_e n_e^2 v_{A\varphi e}^2\right\} - \frac{D_e}{k_{re}}\frac{K_{\nu-1}(k_{re}r_e)}{K_\nu(k_{re}r_e)}\right]$$

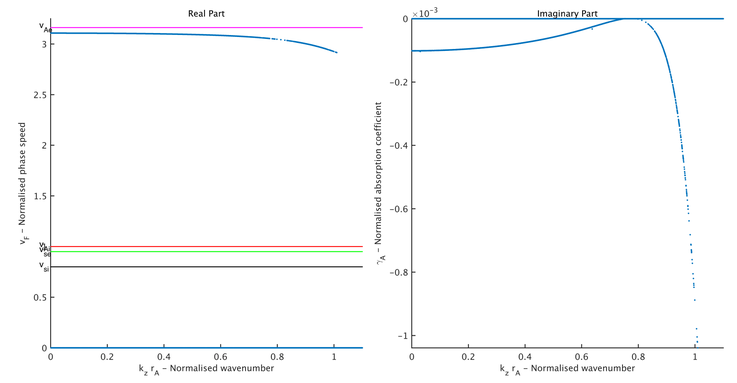

(Left) Normalised phase velocity. (Right) Normalized absorption coefficient. Parameters: Internal temperature (1.000.000 K), external temperature (*400.000 K*), density ratio (internal/external density, *10.0*), magnetic twist $B_\varphi/B_z=0.2$, resonant layer thickness $\delta_A = 0.1r_A$

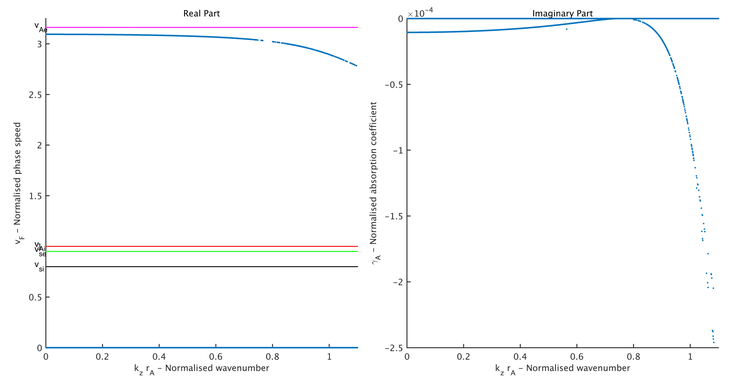

(Left) Normalised phase velocity. (Right) Normalized absorption coefficient. Parameters: Internal temperature (1.000.000 K), external temperature (*400.000 K*), density ratio (internal/external density, *10.0*), magnetic twist $B_\varphi/B_z=0.2$, resonant layer thickness $\delta_A = 0.01r_A$

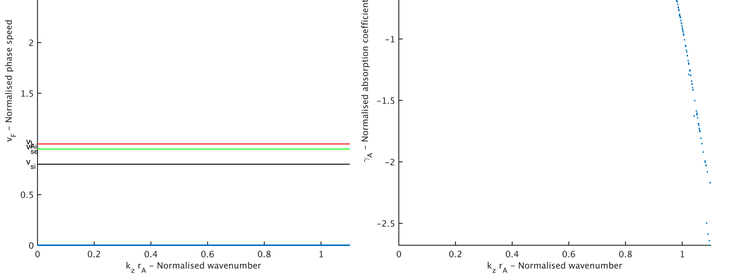

(Left) Normalised phase velocity. (Right) Normalized absorption coefficient. Parameters: Internal temperature (1.000.000 K), external temperature (*400.000 K*), density ratio (internal/external density, *10.0*), magnetic twist $B_\varphi/B_z=0.2$, resonant layer thickness $\delta_A = 0.1r_A$

References

Morton, R. J., Verth, G., Jess, D. B., et al.: Nature Communications, 3, 1315, 2012,
Verwichte, E., Van Doorsselaere, T., White, R. S. & Antolin, P.: Astronomy & Astrophyics,
552, 138, 2013
Fedun, V., Erdélyi, R., Shelyag, S.: Solar Physics, 258, pp. 219-241, 2009
Mumford, S., Fedun, V., Erdélyi, R.:The Astrophysical Journal, 799, 2015
Shelyag, S., Fedun, V., Erdélyi, R.: Astronomy and Astrophysics, 486, pp.655-662, 2008
Vigeesh, G., Fedun, V., Hasan, S. S., Erdélyi, R.: The Astrophysical Journal, 755, pp.id.18, 2012
Fedun, V., Shelyag, S., Verth, G., Mathioudakis, M., Erdélyi, R. *Annales Geophysicae*, 29, pp.1029-1035, 2011